International Journal of Renewable Energy Resources 4 (2014) 35-41

IMPROVED DUAL-AXIS SOLAR TRACKING SYSTEM

M. J. Musa, A. Mohammad, A. Adamu, Y. A. Sha'aban, I. Saleh
Department of Electrical& Computer Engineering, Ahmadu Bello University; Zaria, Nigeria
Technical Skills Acquisition Center Mubi, Adamawa state, Nigeria
Email: mjmusa@abu.edu.ng, mmjibrin@yahoo.com

ABSTRACT
This paper presents techniques for improving dual-axis solar tracking system for maximum energy conversion. The design maintains the solar panel at 90^0 to the solar rays throughout the hours of the day at Zaria, Kaduna state of Nigeria. The system was designed to ensure an automatic control of solar tracking using Light Dependent Resistors (LDRs) attached to both sides of the frame, which houses the solar panel. Tracking motor spin is controlled when the LDRs are exposed to different solar intensity. It was observed that a maximum output voltage of 20.2V was achieved between 8:30am to 5:30pm when the device was used, which has proved the efficiency of solar conversion. The output voltages (V_{01} and V_{02}) from the comparators IC were tested during, motor in stationary position, motor spins in clockwise direction and when the motor spins in anti-clockwise direction to ascertain the system operation. V_{01} and V_{02} were found to obey the theoretical operation of the system by complementing each other at pin1 and pin7 of the dual comparators respectively.

Keywords: Dual-axis, LDR, motor, solar, tracking

1. INTRODUCTION

With the rapid increase in population and economic development, the problems of the energy and global warming effects are today the cause for concern. The utilization of renewable energy sources is the key solution to those problems and one of the renewable sources is solar energy (Saad and Hosni, 2013). Solar energy is the energy extracted from the rays issued from the sun in the form of heat (Kassem and Hamad, 2011). This form of energy is very essential for all life on earth. It is classified as renewable energy source because every day sun rises and falls by nature. Solar energy is economical and less pollution in comparison with other sources of energy (Hemant *et al,* 2011). Solar energy is available in most part of northern Nigeria, although some areas have higher radiation than another (Abdulsalam *et al,* 2012). The sun's radiation is collected and converted into direct current (DC) form of electrical energy with the use of photovoltaic cell or solar panel (Jin-Min and Chia-Liang, 2013). The maximum efficiency of the conversion process is attained when the solar rays are normal (perpendicular) to the solar panel. However, in order to achieve maximum efficiency, solar tracker is used (Saravanan *et al,* 2011).

Solar tracker is an electro-mechanical system, manually or automatically used for orienting photovoltaic panel in perpendicular to the direction of the Sun's rays. The two major classes of solar trackers are single axis solar tracker and dual-axis solar tracker (Kassem and Hamad, 2011). Earlier researchers used single axis tracking system which only follow the sun's east-west movement.

The daily motion of the earth causes the sun to appear in the east and west direction and the annual motion causes the sun to tilt at an angle of 23.5^0 while moving along the east-west direction (Mannan *et al,* 2013). The maximum efficiency of the solar panel cannot adequately be achieved by single axis tracking system. Therefore, to track the sun movement accurately, the use of dual-axis solar tracker is necessary. With the sun's rays always falling at 90^0 to the panel, the maximum energy can be achieved as the panel operates at its greatest efficiency (Hemant *et al,* 2011).

This research paper focused on the dual-axis solar tracking system. The movement of the main frame which houses the solar panel is controlled by two DC motors, one responsible for east-west (EW) movement while the other for north-west (NW) movement. Movement would be achieved by sending signal from a voltage divider network of two LDRs to one of the motors, making a total of four LDR for the two motors.

2. METHODOLOGY

The methodologies used in this research work are electrical unit and mechanical unit. The electrical unit will be discussed on this paper.

2.1 *Electrical Unit*

In order to simplify the design approach, the electrical unit is divided into four subunits as in Figure 1.

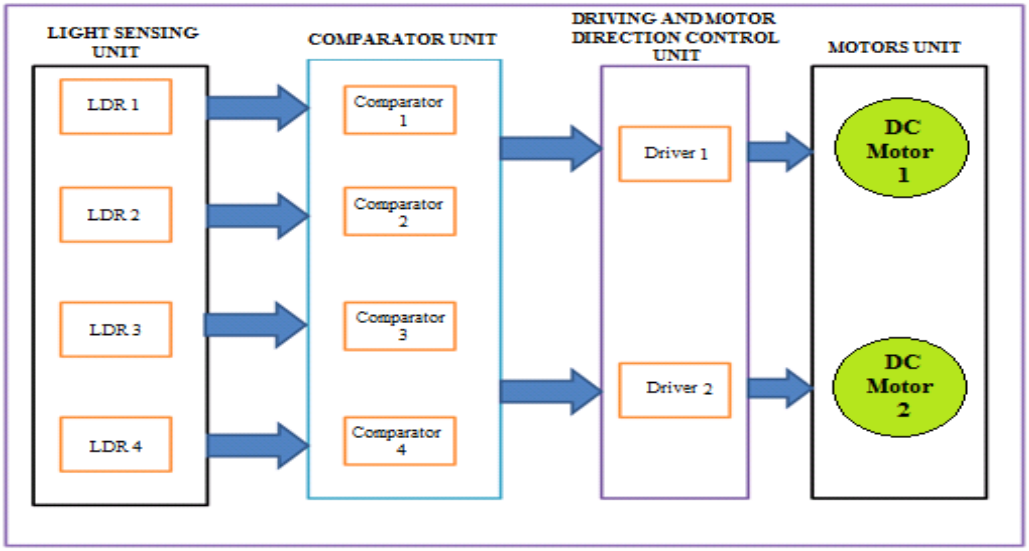

Figure 1 Block Diagram of the Control System.

2.1.1 *Electrical System Design*

The system comprises of two similar hardware electrical circuits, each controlling the bi-directional motion of one of the DC motors, Figure 2 gives one of the similar circuits. The electrical circuit is made up of three modules; the LDR-based sensing unit, the comparators unit and a motor driver (H- Bridge) unit, as in Figure 1.

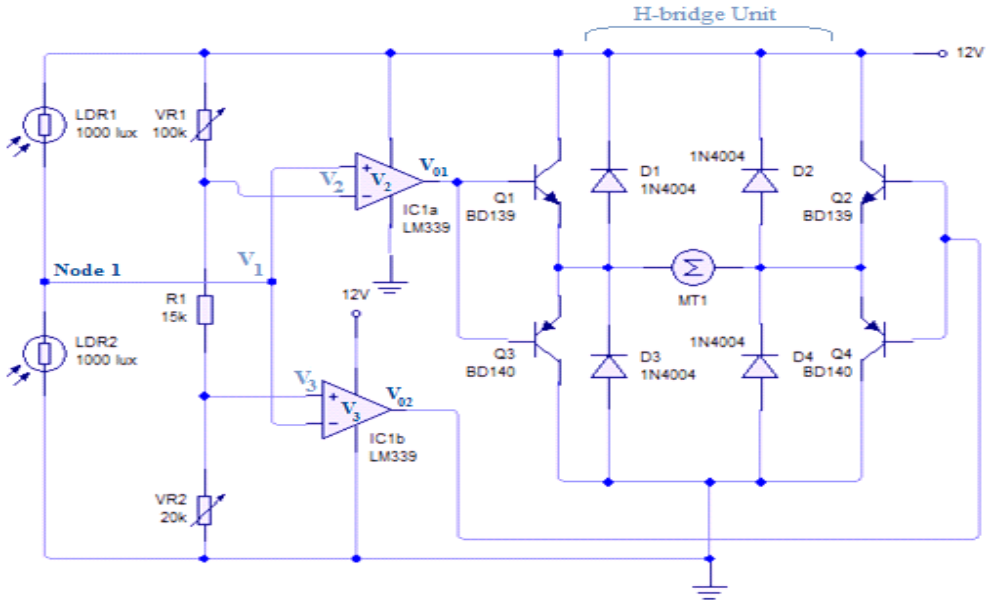

Figure 2 One of the Dual Circuits of the System

2.1.2 *Sensing Unit*

The position of the sun is detected by four (in a group of two) LDR sensors, which are located at the sides of the photovoltaic panel. In the automatic modes, resultant signals from the sensors are fed into a control system that operates a DC motor to tilt the position of the panel until it is perpendicular to the solar rays. LDR_1 and LDR_2 forms voltage divider network, which produces voltage that will be compared with referenced voltage at the input of each comparator as in Figure 2.

As the two LDRs are expected to have equal response to solar rays falling on them, therefore, they are chosen to have the same resistance values.

Applying voltage divider rule at node 1 of Figure 2 (Paul and Winfield, 1989):

$$V_1 = \frac{R_{sb} \times V_{cc}}{R_{sa} + R_{sb}} \quad \textbf{(1)}$$

Where: R_{sa} and R_{sb} are the resistances of the LDR_1 and LDR_2 respectively.

When the LDRs receive the same rays of solar radiation, the value of V_1 is half of V_{cc} then, the outputs of the comparators cannot trigger any of the transistors. The resistance value of the LDR (R_{sa} and R_{sb}) used is $5M\Omega$ each.

$$V_1 = \frac{1}{2} \times V_{cc} \quad \textbf{(2)}$$

For $V_{cc} = 12V, V_1 = 6V$

Where, $\mathbf{V_1}$ is the voltage from the LDRs.

The maximum value of V_1 is obtained when $R_{sb} \gg R_{sa}$ i.e. LDR_1 receives more solar rays than the LDR_2. Then the motor turns in clockwise direction and east to west movement of the solar panel is achieved. If $R_{sa} > R_{sb}$ then the value of V_1 will be:

$$V_1 \angle \frac{1}{2} \times V_{cc} \quad \textbf{(3)}$$

Equation 3 stands when LDR_2 receives higher solar rays than LDR_1 and the motor rotates in anticlockwise direction. Hence the panel rotates from west to east direction.

2.1.3 *Comparators Unit*

The comparator unit is made in such a way that the two comparators are served by a common input voltage (V_1) from the LDRs. The outputs of the comparators are designed to produce voltage levels of 0V ($-V_{cc}$) or (V_{cc})in an alternate mode. Reference voltage limits are set by $\frac{(R+R_{v2})}{(R+R_{v1}+R_{v2})}$ and $\frac{(R_{v2})}{(R+R_{v1}+R_{v2})}$ for IC_{1a} and IC_{1b} respectively.

Using voltage divider rule, the reference voltages were abstained as (Paul and Winfield, 1989):

$$V_2 = \frac{R + R_{V2}}{(R + R_{V1} + R_{V2})} \times V_{cc} \quad \textbf{(4)}$$

$$V_3 = \frac{R_{V2}}{(R \quad + R_{V1} + R_{V2})} \times V_{cc} \quad \textbf{(5)}$$

Where, V_2 is the reference voltage for comparator1, V_3 is the reference voltage for comparator 2.

The voltage levels to trigger the motor to either direction is when V_{01} and V_{02} are 90% and 12% of V_{cc} respectively or vice vercer. To achieve this, the V_{IN} has to be $\frac{1}{2}V_{cc}$, which is about 6V and the reference voltages V_2 and V_3 are 25% and 14% of V_{cc} (2.98V and 1.69V) respectively. If the maximum current drawn by the sensitivity resistors is assumed to be approximately 85µA, the resistors values can be calculated as (Paul and Winfield, 1989):

$$R_{V2} = V_3 / I_{DIV} \quad \textbf{(6)}$$

Where: I_{DIV} is the current of the voltage divider network.

$R_{v2} \approx 20k\Omega$

$$R + R_{v2} = V_2 / I_{DIV} \quad \textbf{(7)}$$

$R = 15k\Omega$

By the application of KVL around the loop (Paul and Winfield, 1989):

$$\boldsymbol{V_{R_{v1}} = V_{cc} - V_2 - V_3} \quad \textbf{(8)}$$

$V_{R_{v1}} = 7.33V$

$$R_{v1} = V_{RV1} / I_{DIV} \quad \textbf{(9)}$$

$R_{v1} = 86235.29\Omega$

Standard value of 100kΩ was used as R_{v1}.

Output of IC_{1a} is low when voltage V_1 is less than V_2, otherwise it is high. Output of IC_{1b} is low when voltage V_1 is greater than V_3, otherwise it is high.

2.1.4 *Design of H- bridge (driver) Unit*

H-bridge is a circuit designed to drive the motor into bidirectional motion as in Figure 2 of section 2.1.1. It is done in such away that a combination of two transistors (Q_1 and Q_4) should trigger the motor in one direction while the other combination (Q_2 and Q_3) to the other direction. Chosen of transistors are made on the bases that the outputs of V_{01} and V_{02} of the two comparators are to swing between a low (0.43V) and a high (11.86V) voltage levels, to alternately activate the corresponding transistors for the motor to spins clockwises or other wise.

2.1.5 *Prime Mover (DC motor)*

Two identical 12V DC motors of no-load speed: 33rpm, load torque: 3.5Nm were used in driving the system into the dual axis tracking. From the make, the motor has the following parameters.

The equations of motion for DC motors are (Austin, 2006):

$$V = L\frac{di}{dt} + IR + K_b \dot{\theta} \quad \textbf{(11)}$$

$$M\ddot{\theta} = IK_T - V\dot{\theta} - \tau \quad \textbf{(12)}$$

Where:

V is the voltage applied to the motor,
L is the motor inductance,
I is the current through the motor windings,
R is the motor winding resistance,
K_b is motor's back electro magnetic force (e.m.f) constant,
$\dot{\theta}$ is the motor's angular velocity,
M is the rotor's moment of inertia,
K_T is the motor's torque constant,
ν is motor's viscous friction constant,
τ is torque applied to rotor by an external load.

2.2 *Operational Principle of the System*

The system operates in the following principles;

i. It is to be installed at a place where it will not be not be covered by any shadow from 8:30AM to 5:30PM daily to ensure a total exposure to solar rays.
ii. Refference voltages (V_2 and V_3) for comparators "A" and "B" respectively, are set by variable resistors R_{V1} and R_{V2} through a voltage divider network.
iii. For the solar panel to remains parpendilar to the solar rays, all the LDRs should be exposed to the same level of illumination.

iv. When a difference in the illumination is experienced by the LDRs, a voltage V_1 is developed from the voltage divider network of the LDRs.

v. V_1 served as input voltage at Non-inverting terminal of comparator "A", at the same time, an input voltage at the Inverting terminal of comparator "B".

vi. If $V_1 > V_2$, the output (V_{01}) of comparator "A" goes high (approximately equal to V_{CC}) which put transistor Q_1 into conduction (saturation state) , thereby allowing the supply voltage V_{CC} to reach the terminal of the motor. On the other hand, $V_1 > V_3$, the output (V_{02}) of comparator "B" goes low (in this case, to about 1.43V), which is only enough to put transistor Q_4 into conduction. Thereby allowing the other terminal of the motor to have access to ground. Under this condition, the motor spins in clockwise direction untill the two LDRs are exposed to the same illumination level.

vii. When $V_1 < V_2$ and $V_1 < V_3$, the process of step 6 is reversed. i.e. V_{01} goes low and V_{02} goes high. Putting Q_3 and Q_2 to conduct, which makes the motor to spins in anti-clockwise direction untill the two LDRs are exposed to the same illumination level.

viii. With the repeat of step 6 and/or 7, the tracking process is manitained from sun rise to sun set.

3. RESULTS AND DISCUSSION

Simulated and measured results were peresented and compared to accertain the conformity of the system. Measurements were taken when the pannel is at fixed position, single axis tracking and dual-axis tracking.

3.1 *Simulation Test*

The control circuit was simulated using a circuit wizard software and the results of the simulation test were presented in table 1.

Table 1 Simulation Values of Control Circuit

	Voltage at Different Points (V)						
Motor Satatus	**V_{cc}**	**V_1**	**V_2**	**V_3**	**V_{01}**	**V_{02}**	**V_m**
Stationary	12.00	6.00	6.12	2.73	0.24	0.24	0.00
Spins Clockwise	11.89	6.47	6.06	2.70	0.51	10.68	9.83
Spins Anti-clockwise	11.89	11.26	6.06	2.71	10.67	0.45	9.73

3.2 *Measurement Voltages*

Direct measurements was carried out at various points using multimeter (corresponding to the points observed in simulation test) on the completed control circuit and table 2 readings were obtained. Table 3 presents the difference between the simulated values and measured values.

Table 2 Measured Values from Control Circuit

	Voltage at Different Points (V)						
Motor Satatus	**V_{cc}**	**V_1**	**V_2**	**V_3**	**V_{01}**	**V_{02}**	**V_m**
Stationary	12.20	6.92	6.17	3.55	0.00	0.00	0.00
Spins clockwise	11.80	6.55	6.71	3.46	0.84	10.44	9.65
Spins anti-clockwise	11.75	11.60	6.91	3.10	10.50	0.75	9.73

Where: V_m is the at the motor terminals.

Table 3 Differences Between Measured and Simulated Values of Control Circuit

	Differences Betweeen the Measured and Simulated Values (V)						
Motor Satatus	**V_{ccd}**	**V_{1d}**	**V_{2d}**	**V_{3d}**	**V_{01d}**	**V_{02d}**	**V_{mds}**
Stationary	0.20	0.92	0.05	0.82	-0.24	-0.24	0.00
Spins clockwise	-0.09	0.08	0.11	0.76	0.33	-0.24	-0.18
Spins anti-clockwise	-0.14	0.34	0.85	0.39	-0.17	0.30	0.00

The above table of differences between the measured and simulated values has shown that, there is high conformity between the values obtained, since the differences are very negligible and has proved a very good level of accurracy of the work.

3.3 *Complete System Test*

The complete system has the experimental advantages to be use as fixed panel position solar system when all the motors are deactivated, can used as single axis solar tracker when one of the motor is deactivated and then

as the dual-axis tracker. The three conditions were used and the following results were obtained. The constructed control panel and the complete system is shown on plate 1 and 2 respectively. The size of thecase was made portably small and allowing room for ventilation.

Figure1 Control System in Cassing (Plate 1)

Figure2 Complete System (Plate 2)

3.3.1 *Panel used as Fixed Position*

It was obseved that, when a solar panel is kept at fixed position, an angle of 25^0 South-East (SE) gives the best output. Based on this, tests were carried out and results were presented on table 4.

Table 4 Output of a Fixed Position Panel

Time of the Day (hrs)	Output Voltage (V)	Output Current (A)	Output Power (W)
8:30am	20.04	3.64	73.07
9:30am	20.10	3.63	72.96
10:30am	20.11	3.62	72.80
11:30am	20.10	3.59	72.16
12:30pm	20.10	3.59	72.16
1:30pm	17.95	3.60	64..62
2:30pm	17.76	3.61	64.11
3:30pm	15.65	3.78	59.16
4:30pm	10.02	3.91	39.18
5:30pm	8.04	3.96	31.84

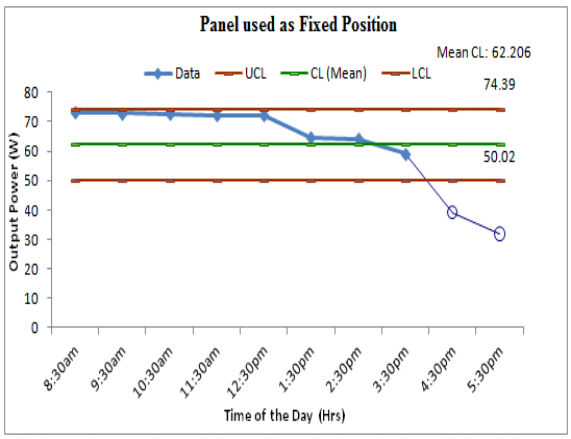

Figure 3 Shows the Induvidual Chart of Power for Fixed Position

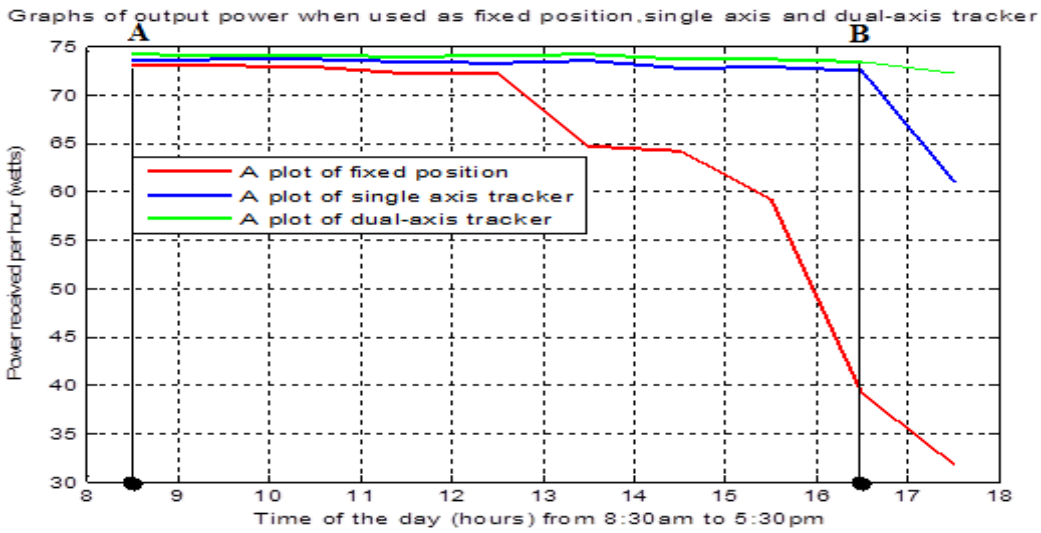

Figure 4 The Induvidual Chart of Power for Single-axis Tracking System

It is clearly shown from Figure 3 that the mean centerline (CL) value is 62.206W only with two points below lower control limit (LCL) and five values at. upper control limit (UCL), this proved the inefficiency of fixed pannel possition. From Figure 4, the mean value is 71.975W and has a reading below the LCL this value proves an improvement in the performance of the single-axis tracking system over the fixed panel position.

3.3.2 *Panel used as Single-axis Tracking System.*
The motor for south-north (SN) motion was deactivated, which made the system behaved as single axis solar tracker and table 5 readings were obtained. From Figure 2, the mean value is 71.975W and has a reading below the LCL this value proves an improvement in the performance of the single-axis tracking system over the fixed panel position.

3.3.3 *Panel used as Dual-axis Tracking System*
When the two motors are active, the system behaved normally as dual-axis solar tracker. Table 6 presents the measurements. Figure 5 shows the dual-axis tracking system with mean value of 73.687W and a single value below the LCL this proves most improved tracking system as compare to the fixed and single tracking system. Figure 6 shows the comparison of power agains time from the three tables 4, 5 & 6.

Table5 Measured Output when used as a Single-axis Tracker

Time of the Day (hrs)	Output Voltage (V)	Output Current (A)	Output Power (W)
8:30am	20.09	3.67	73.53
9:30am	20.10	3.66	73.57
10:30am	20.11	3.66	73.60
11:30am	20.10	3.65	73.37
12:30pm	20.10	3.64	73.16
1:30pm	20.09	3.66	73.53
2:30pm	20.04	3.63	72.75
3:30pm	20.00	3.64	72.80
4:30pm	19.86	3.65	72.49
5:30pm	16.34	3.73	60.95

3.3.4 *Comparison with Similar Work*
The findings of this paper will now be compared with the recent similar work presented by Jay-Robert *et al*, (2014), tilled: Optimization of a small scale dual-axis solar tracking system using nano-watt technology. In the effort to optimized dual-axis solar tracking system, Figure 7 was presented as a comparison between fixed panel and tracking panel system. It can be read from the Figure 7 that the maximum power achieved can only be maintained for 4hrs (from A' *to* B' on time axis). Moreover, Figure 6 indicated the improvement of dual axis solar tracker, which maintained maximum power achieved for 8hrs. panel and tracking panel system. It can be read from the Figure 7 that the maximum power achieved can only be maintained for 4hrs (from A^' to B^' on time axis). Moreover, Figure6 indicated the improvement of dual axis solar tracker, which maintained maximum power achieved for 8hrs.

4. CONCLUSION
The results obtained in tables 1, 2, have proved that for the motor to remains in a stationary position, V01 & V02 should be very low and this kept the Q1 & Q2 transistors in cut-off states. While, for the motor to

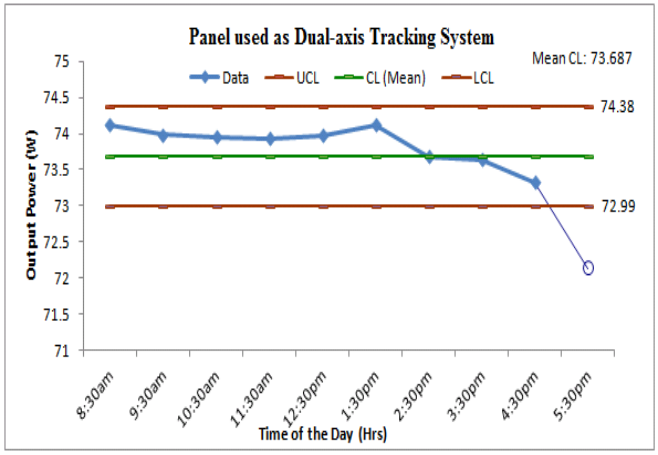

Figure 5 The Induvidual Chart of Power for Dual-axis Tracking System

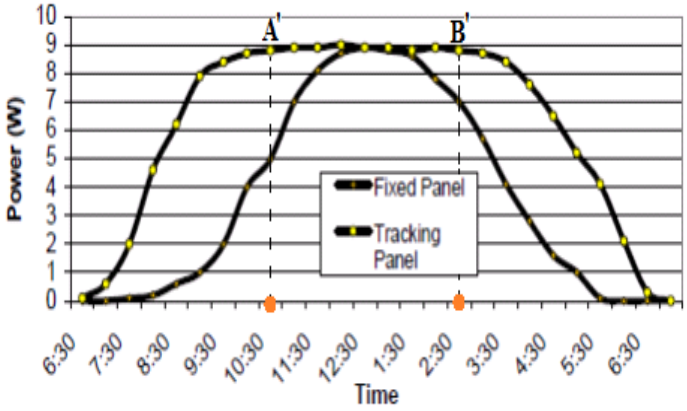

Figure 6 Comparison of Fixed, Single and Dual-axis Tracker

Table 6 Measured Output when used as Dual-aixs Tracker

Time of the Day (hrs)	Output Voltage (V)	Output Current (A)	Output power (W)
8:30am	20.14	3.68	74.12
9:30am	20.16	3.67	73.99
10:30am	20.15	3.67	73.95
11:30am	20.20	3.66	73.93
12:30pm	20.21	3.66	73.97
1:30pm	20.14	3.68	74.12
2:30pm	20.13	3.66	73.68
3:30pm	20.12	3.66	73.64
4:30pm	20.09	3.65	73.33
5:30pm	19.34	3.73	72.14

spins clockwise or anti-clockwise the voltages V_{01}& V_{02} should complemented one another. The values rialized in tables 4, 5 & 6 has shown that the output power of a dual-axis solar tracking system has an improvement in performance efficiency over fixed position and single axis solar tracker as compared in Figure 6. Moreover, the improvement of the dual-axis was shown as compired with latest similar work.

REFERENCE

Abdulsalam, D., Mbamali, I. and Mamman, M. 2012. An Assessment of Solar Radiation Patterns for Sustainable Implementation of Solar Home Systems in Nigeria. American International Journal of Contemporary Research: Zaria, Nigeria 6(2).

Applied Research in Mechanical Engineering, Uttar Pradesh, India (1).

Austin, H. 2006. Electric Motors and Drivers (Third ed.) published by Elsevier Ltd. Linacre House, Jordan Hill, Oxford OX2 8DP 30 Corporate Drive, Suite 400, Burlington, MA OI803.

Hemant, K., Manoj, K., Nagendra, P. and Rashmi, R. 2011. Fabrication and Experimental Study on Two-Axis Solar Tracking. International Journal of

Jay-Robert, B.R., Reggie, C.G. and Elmer, P.D. 2014. Optimization of a Small Scale Dual-Axis Solar Tracking System using Nanowatt Technology. Journal of Automation and Control Engineering Vol. 2, No. 2

Jing-Min, W. and Chia-Liang, L. 2013. Design and Implementation of a Sun Tracker with a Dual-Axis Single Motor for an Optical Sensor-Based Photovoltaic System. Sensors journals, Tamsui District, New Taipei City 25135, Taiwan.

Kassem, A. and Hamad, M. 2011. A microcontroller-based multi-function solar tracking system: Notre Dame University Louaize. Department of Electrical and Computer and Communication Engineering.

Mannan, M., Sanzidur, R., Rashid, A. and Mahir, A. 2013. Design & Implementation of a Dual Axis Solar Tracking System. American Academic & Scholarly Research Journal, American international university, Bangaladesh. 1(5)

Paul, H. and Winfield, H. 1989. The Art of Electronics (Second ed.), Cambridge University Press, ISBN 978-0-521-37095-0

Saad, D.O. and Hosni, I.A. 2013. Design and development of an educational solar tracking parabolic trough collector system. Global Journal of Engineering Education. Volume 15

Saravanan, C., Panneerselvam, M. and Christopher, I. 2011. A novel low cost automatic solar tracking system. International Journal Computer Applications.